Available online at www.sciencedirect.com
ScienceDirect
Journal of Magnetic Resonance 187 (2007) 357–362
JMR Journal of Magnetic Resonance
www.elsevier.com/locate/jmr

Communication

Double spin-echo sequence for rapid spectroscopic imaging of hyperpolarized ^{13}C

Charles H. Cunningham [a,*], Albert P. Chen [b], Mark J. Albers [b], John Kurhanewicz [b], Ralph E. Hurd [c], Yi-Fen Yen [c], John M. Pauly [d], Sarah J. Nelson [b], Daniel B. Vigneron [b]

[a] *Department of Medical Biophysics, Sunnybrook Health Sciences Centre, 2075 Bayview Ave., Toronto, Ont., Canada M4N 3M5*
[b] *Department of Radiology, University of California at San Francisco, San Francisco, CA, USA*
[c] *GE Healthcare Technologies, Menlo Park, CA, USA*
[d] *Department of Electrical Engineering, Stanford University, Stanford, CA, USA*

Received 2 February 2007; revised 17 April 2007
Available online 2 June 2007

Abstract

Dynamic nuclear polarization of metabolically active compounds labeled with ^{13}C has been introduced as a means for imaging metabolic processes *in vivo*. To differentiate between the injected compound and the various metabolic products, an imaging technique capable of separating the different chemical-shift species must be used. In this paper, the design and testing of a pulse sequence for rapid magnetic resonance spectroscopic imaging (MRSI) of hyperpolarized ^{13}C is presented. The pulse sequence consists of a small-tip excitation followed by a double spin echo using adiabatic refocusing pulses and a "flyback" echo-planar readout gradient. Key elements of the sequence are insensitivity to calibration of the transmit gain, the formation of a spin echo giving high-quality spectral information, and a small effective tip angle that preserves the magnetization for a sufficient duration. Experiments *in vivo* showed three-dimensional coverage with excellent spectral quality and SNR.

Keywords: ^{13}C; Hyperpolarized; Pyruvate; Spectroscopic imaging; MRSI

1. Introduction

Hyperpolarization of metabolically active compounds labeled with ^{13}C has been recently reported as a means for imaging metabolic processes *in vivo* [1–3]. With the use of the chemical shift of the ^{13}C nucleus to distinguish between different molecular structures, separate images can be made of the injected compound as well as its metabolic products. This methodology holds great promise for gaining insight into changes in cellular metabolism when diseases such as cancer are present, and for potentially using these changes for diagnosis.

To differentiate between the injected compound and the various metabolic products, an imaging technique capable of separating the different chemical-shift species must be used. In addition, the fact that the hyperpolarized spins are decaying during the data acquisition and are not replenished by T_1 recovery necessitates careful pulse sequence design.

In this paper, we present the design and testing of a pulse sequence for rapid magnetic resonance spectroscopic imaging (MRSI) of hyperpolarized ^{13}C that is robust to tip-angle errors. The pulse sequence consists of a small-tip excitation followed by a double spin echo using adiabatic refocusing pulses and a "flyback" echo-planar readout gradient. The performance of the sequence is demonstrated with phantom experiments and an *in vivo* experiment with hyperpolarized pyruvate injected into a live rat showing

* Corresponding author. Fax: +1 416 480 5714.
E-mail address: chuck@sri.utoronto.ca (C.H. Cunningham).

1090-7807/$ - see front matter © 2007 Elsevier Inc. All rights reserved.
doi:10.1016/j.jmr.2007.05.014

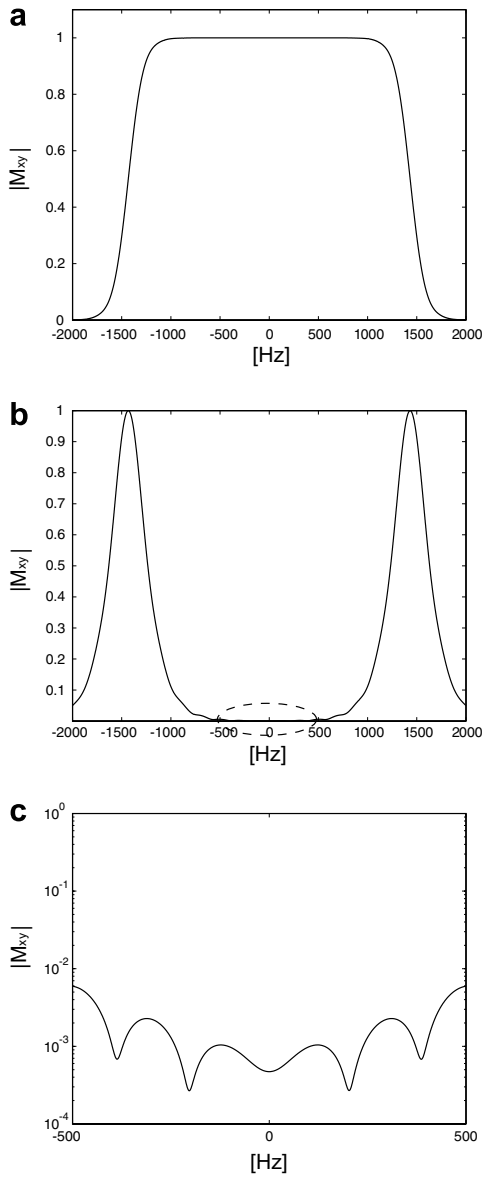

Fig. 1. Performance of the hyperbolic-secant refocusing pulses. (a) The crushed spin-echo profile ($M_{xy} \rightarrow M_{xy}$) shows a refocused bandwidth of 2.8 kHz. (b) The excitation profile ($M_z \rightarrow M_{xy}$) of the pulse shows that the fraction of z-magnetization that is tipped to the transverse plane is negligible over a range of 1 kHz. (c) A zoomed view is shown of the region in the dashed circle on (b).

metabolism of the injected compound in a variety of tissues.

2. Theory

Pulse sequences for manipulating hyperpolarized samples must be designed to accommodate the fact that magnetization is not replenished through T_1 relaxation. In the experiments presented below, the magnetization must be preserved over 96 separate excitations so that enough phase encodes are acquired to reconstruct the three-dimensional volume. The strategy used for these experiments was to tip only a small fraction of the magnetization into the transverse plane for each data acquisition [4,5]. However, a spin-echo signal was desired to cope with magnetic field inhomogeneities and to allow phase-sensitive spectral reconstruction. Applying a single, conventional 180° refocusing pulse after a small-tip excitation was not a possibility as this would be unacceptably sensitive to miscalibration of the transmit gain. Accurately, setting the transmit gain is non-trivial because the data acquisition must be started immediately after injection of the hyperpolarized compound.

In order to achieve a spin echo with a small net tip angle, we propose the use of a "double spin echo" sequence [6,7]. This sequence consists of a small-tip excitation followed by a pair of adiabatic refocusing pulses so that the magnetization is tipped back near the positive z-axis before each data acquisition. Errors in transmit-gain calibration will only affect the small-tip portion of the sequence, since the adiabatic refocusing pulses are designed to give the same rotation angle over a range of $B1$ amplitudes. By using a pair of adiabatic pulses,the non-linear phase across the spectrum that would result from a single pulse is re-wound [8].

Previous applications of the low-tip, double spin-echo sequence [6,7] have been intended to avoid the increased rate of signal loss that occurs due to T_1 decay when the magnetization is opposed to the main magnetic field. The value of T_1 for a material is the same whether the spins are hyperpolarized or at thermal equilibrium. However, the behavior of hyperpolarized magnetization is different in that its magnitude decays at the same rate whether inverted or upright. This is because the equilibrium magnetization is negligible relative to the hyperpolarization. However, there is another important reason

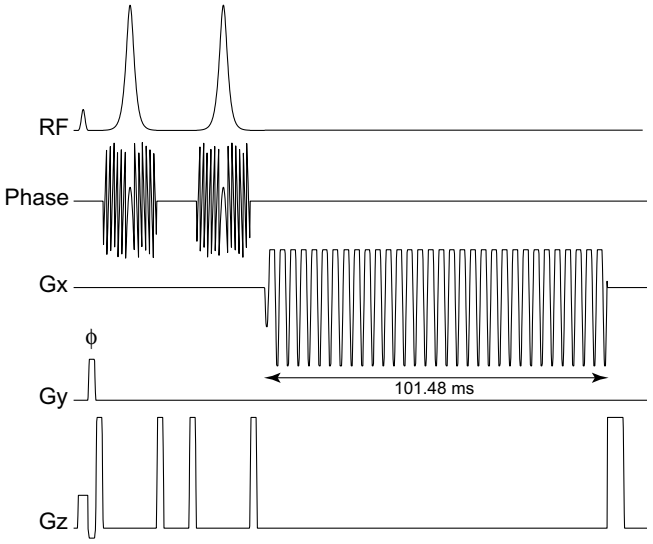

Fig. 2. Timing diagram of the double spin-echo pulse sequence. The echo-planar readout gradient gives a spectral bandwidth of 581.4 Hz and a maximum spatial resolution of 5.4 mm (for ^{13}C). Spatial encoding in the y- and z-dimensions is accomplished with phase-encoding gradients at the time indicated by the ϕ symbol.

to leave the hyperpolarized magnetization along the positive z-axis after each repetition. Magnetization that is not affected by the RF pulses, either because it is outside the active area of the RF coil or outside the selected slice (in the case where the adiabatic pulses are played in the presence of a gradient) will remain along the $+z$-axis and these spins could flow into the volume being imaged. If the magnetization in the imaging volume were periodically inverted, mixing with the non-inverted magnetization flowing into this volume could cause rapid loss of polarization.

3. Methods and results

The adiabatic refocusing pulse was designed and tested in MATLAB™ (The Mathworks Inc., Natick, MA). The pulse envelope and phase waveform were computed using the analytic expression derived by Silver and Hoult [9]:

$$B1(t) = A\,\mathrm{sech}(\beta t)\mathrm{e}^{\mathrm{i}\mu\log(\mathrm{sech}(\beta t))} \quad (1)$$

with $\beta = 7.5$, $\mu = 8$, and t running from -1 to 1 in discrete steps to give 2500 samples. The amplitude A was set to give a maximum RF field strength of 0.17 mT with a pulse duration of 10 ms. The pulse parameters were chosen through iterative Bloch-equation simulations to compute the fraction of longitudinal magnetization that will be converted to transverse magnetization by the pulse (this value would ideally be 0 over the desired bandwidth). The performance of the final design of the pulse is shown in Fig. 1.

The source code for a free induction decay (FID) MRSI pulse sequence was modified to incorporate the adiabatic refocusing pulse shown in Fig. 1 and a flyback echo-planar readout gradient during the data acquisition. The timing diagram for the new pulse sequence is shown in Fig. 2. The first, low-tip pulse is a sinc-like slab-select pulse designed with the Shinnar–Le Roux algorithm [10]. Experiments were performed on a General Electric EXCITE 3 T (Waukesha, WI) clinical MRI system equipped with 40 mT/m, 150 mT/m/ms gradients and a broadband RF amplifier. A custom built, dual-tuned rat birdcage coil was used for RF transmission and signal reception. For the experiments with hyperpolarized solution, the transmitter gain was set based on measurements from prior

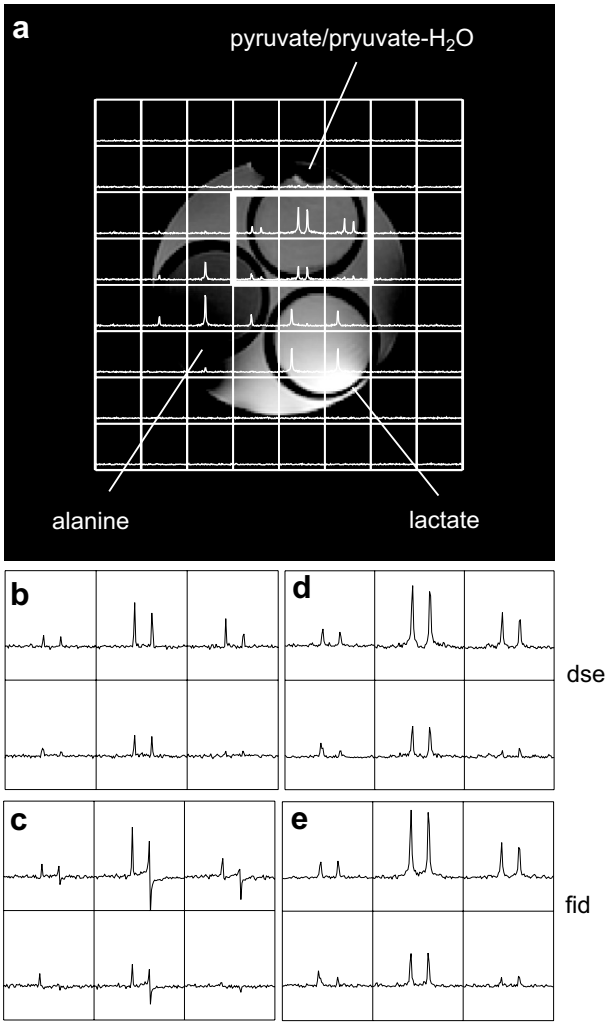

Fig. 3. Comparison to conventional pulse-acquire sequence in a phantom experiment. The tip angle is the same for both sequences (10°). Spectra from the six voxels indicated by the thick lines on the proton image (a) are shown in (b–e). Phase-sensitive spectra for the two sequences are shown in (b) and (c). The magnitude of these two spectra are shown in (d) and (e). Note the linear phase across the spectrum in (c) due to the lack of a spin echo. The peak magnitudes in (d) are slightly smaller than in (e), presumably because of T_2 decay.

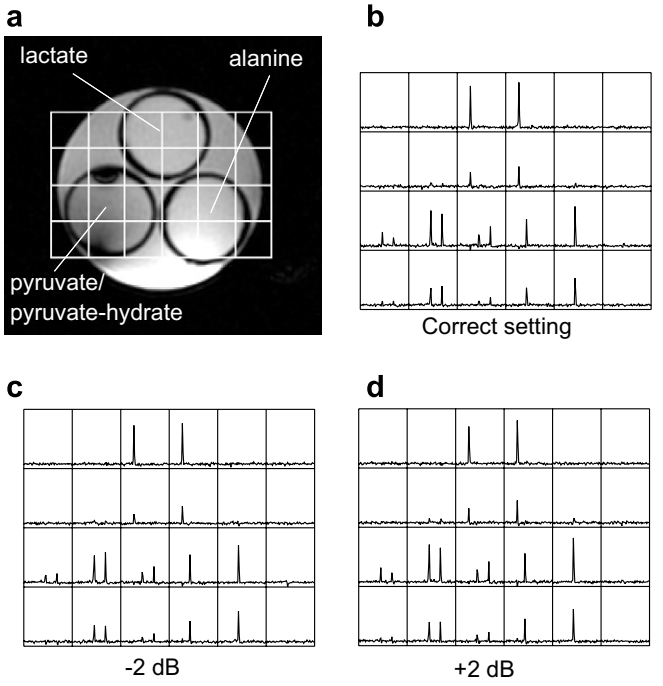

Fig. 4. Demonstration of the insensitivity of the pulse sequence to miscalibration of the transmit gain. (a) The grid shows the locations of the voxels within the phantom. (b) Spectra acquired with the correct transmit gain setting. (c and d) Gain mis-set to be reduced and increased by 2 dB, respectively. Note that the peak heights are similar despite a ±26% change in RF amplitudes.

phantom experiments and was estimated to be accurate to ±10%.

For all experiments, data for a three-dimensional volume were acquired by phase encoding in two spatial dimensions and using the echo-planar readout gradient in the third dimension, resulting in k-space sampling on a Cartesian grid. A linear phase correction was applied in the spectral dimension associated with the different sampling times for each of the points acquired on the plateaus of the flyback readout gradient. The correction was computed as in [11] (after the Fourier transform in the time dimension but before the spatial transform). Other than this, the data were processed as a standard chemical-shift imaging (CSI) data set [12].

Phantom studies were performed to verify that the behavior of the signal under T_1 relaxation was the same with the double spin-echo sequence as compared with a single, small tip. The comparison was made with an MRSI pulse sequence consisting of a single small-tip pulse immediately followed by data acquisition. Data were acquired from a spherical phantom consisting of smaller, inner spheres containing enriched samples of $^{13}C_1$-labeled pyruvate, lactate and alanine. This phantom measurement was sensitive to tip angle because the T_1s of the ^{13}C nuclei in these compounds, at the C_1 position in each molecule, was long compared to the TR used ($T_1 \approx 10$ s and TR = 250 ms). The results of this phantom experiment are shown in Fig. 3. The insensitivity of the pulse sequence to mis-calibration of the transmit gain was demonstrated using this same phantom, by acquiring spectra with the gain mis-set by ±2 dB. As seen in Fig. 4, there is still a slight difference in tip angle at the different gain settings since the first, selective RF pulse is not adiabatic. However, since this is a small-tip pulse, a 10% error in the gain only results in a 1° error in tip angle. The advantage of using a spin-echo sequence can be seen in Fig. 3b where the line-

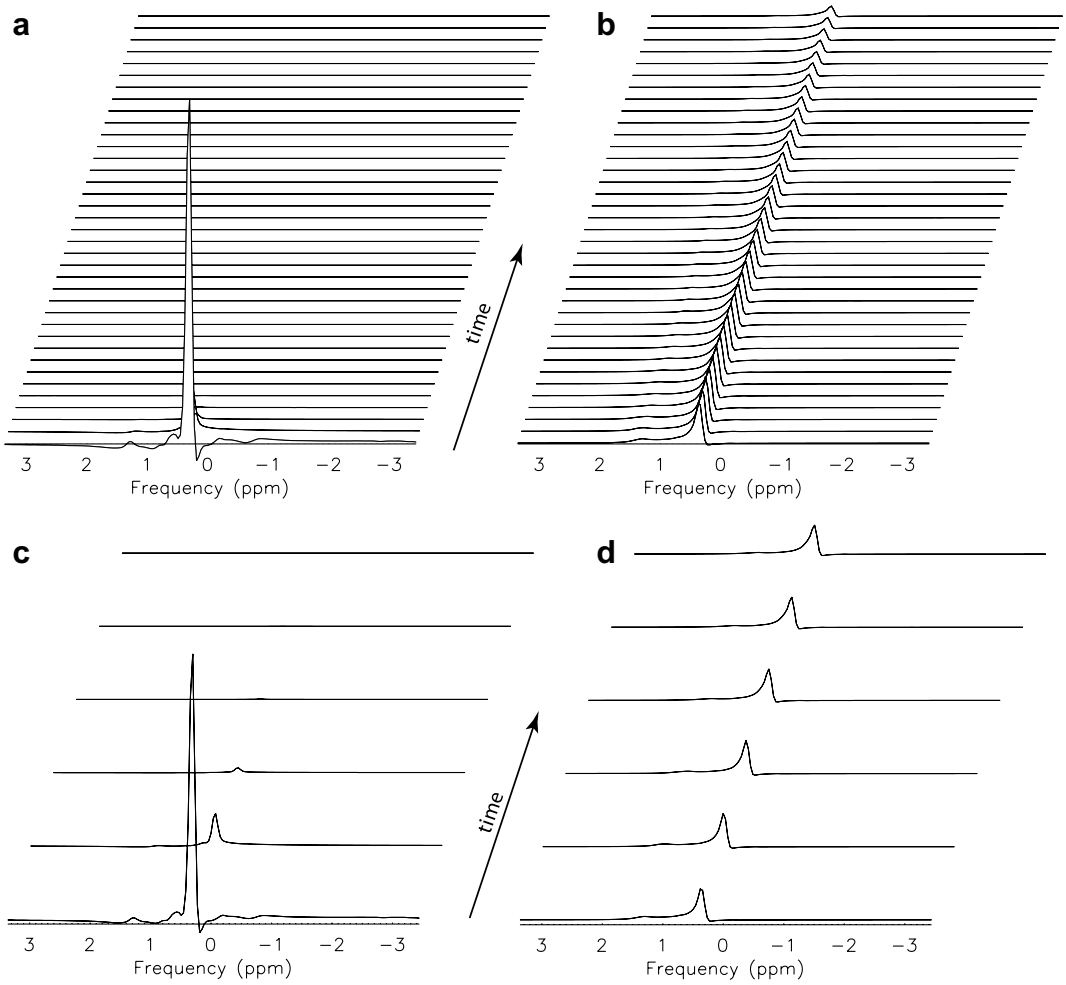

Fig. 5. Phantom experiment demonstrating that the hyperpolarization is preserved over many excitations using the double spin-echo sequence. The spectra show a single peak (corresponding to pyruvate) resolved every 3 s. (a) The first 36 (of 96) spectra with a nominal tip angle of 90° shows rapid signal loss. (b) Using a 5° tip angle, the signal is preserved for many excitations. (c) The first 6 spectra from (a) show that the tip angle is slightly different that 90° (since there is residual magnetization after the first excitation) and that the signal is almost completely lost by the 5th excitation. (d) The corresponding subset from (b) shows steady signal amplitude.

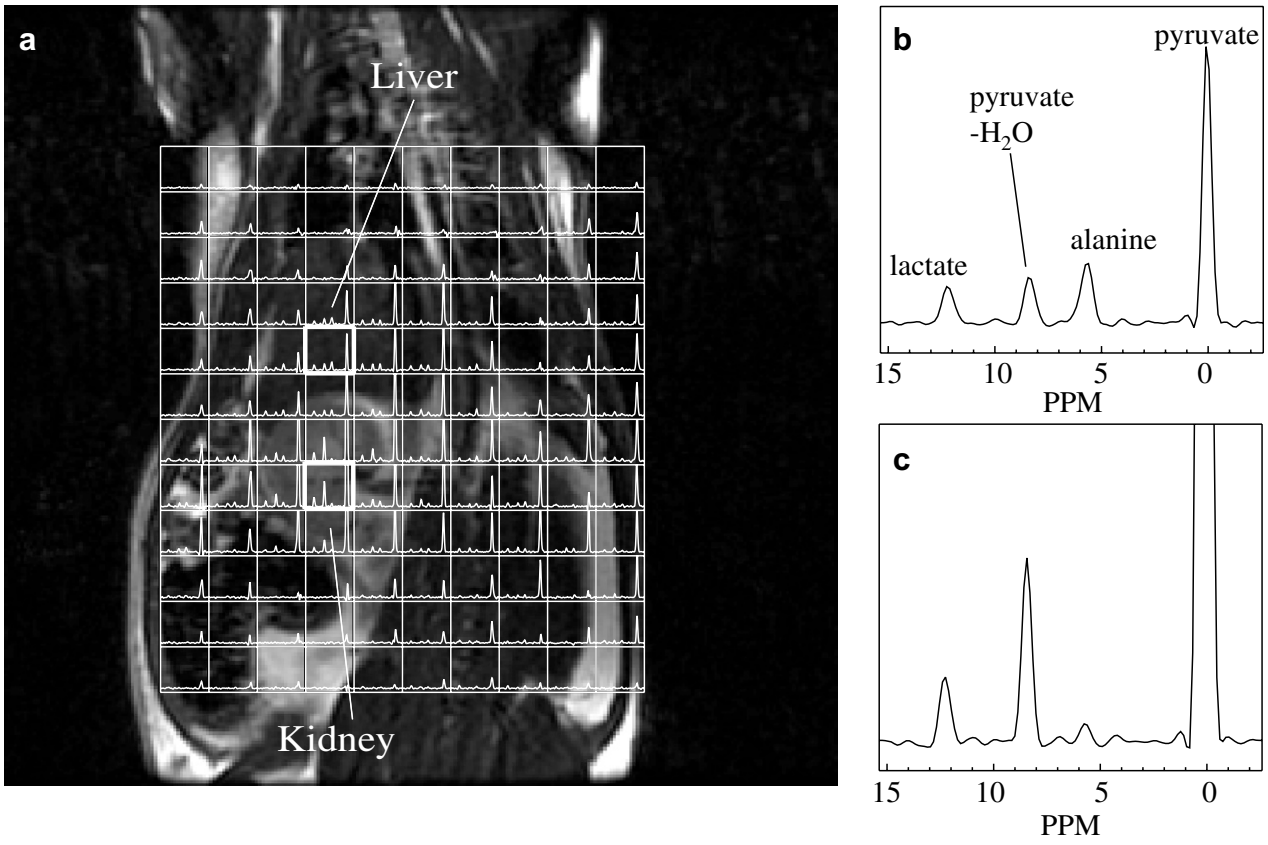

Fig. 6. *In vivo* experiment demonstrating the spectral quality and the conversion of hyperpolarized media into downstream metabolic products. (a) An array of the spectroscopic imaging voxels are shown on top of a coronal T_2-weighted image, indicating voxel locations. (b) Spectrum from a voxel containing liver tissue shows lactate and alanine in similar concentrations. (c) Spectrum from kidney tissue shows elevated lactate. The acquisition parameters were $12 \times 8 \times 16$ spatial encoding with the echo-planar gradient in the z-dimension, 7 mm isotropic spatial resolution, TE = 35 ms, TR = 160 ms, total scan time = 15.4 s, total data sampling time = 9.7 s.

widths are half the width of the magnitude spectra in (d) and (e) and the linear phase seen (c) is refocused, greatly simplifying quantification.

To demonstrate that the double spin-echo sequence enables preservation of the hyperpolarization over the many excitations necessary for three-dimensional imaging, a phantom experiment was performed. A 45 mg sample of pyruvic acid was hyperpolarized in the solid state and dissolved by 6 mL of heated solvent. The solution was immediately transferred to a 5-mL syringe and placed in the birdcage coil. The pulse sequence of Fig. 2 was run with the nominal tip angle of the first, selective RF pulse set to 5°. No phase encoding was applied so that the signal dynamics could be observed. A second sample of pyruvic acid was hyperpolarized and the procedure was repeated with a nominal tip angle of 90°. The results of this experiment are shown in Fig. 5.

For the *in vivo* experiment, the dynamic nuclear polarization (DNP) and dissolution method [13] was used to achieve ~15% polarization of $^{13}C_1$-pyruvate in the solution state. The sample was rapidly dissolved to a concentration of 250 mM. Polarization was estimated by extracting a small aliquot of the dissolved solution and injecting it into a capillary tube within a custom-designed low field NMR spectrometer to provide measurements of FIDs. An injection of 3.6 mL of the hyperpolarized solution into the tail vein of a 510 g Sprague–Dawley rat was made 25 s prior to the start of the data acquisition. All animal studies were carried out under a protocol approved by the UCSF Institutional Animal Care and Use Committee. The data from this experiment are shown in Fig. 6. Although direct computation of the concentrations based on the area under each peak would be difficult because of the unknown magnetization of the injectate by the time it gets to the imaging volume, a ratio of peak areas could be used to give quantitative, localized measurements.

4. Conclusions

In conclusion, we have developed a simple and robust pulse sequence for rapid three-dimensional MRSI of hyperpolarized $^{13}C_1$-pyruvate and its downstream metabolic products. Key elements of the sequence are insensitivity to calibration of the transmit gain, the formation of a spin echo giving high-quality spectral information, and a small effective tip angle that preserves the magnetization for a

sufficient duration. Experiments *in vivo* showed three-dimensional coverage with excellent spectral quality and SNR.

Acknowledgments

The authors are grateful for support from NIH grants R21 EB005363, R01 CA111291 and R01 EB007588.

References

[1] K. Golman, R. Zandt, M. Thaning, Real-time metabolic imaging, Proc. Natl. Acad. Sci. USA 103 (2006) 11270–11275.

[2] A.P. Lin, T.T. Tran, P. Bhattacharya, K. Harris, B.D. Ross, Fast chemical shift imaging of hyperpolarized ^{13}C substrates, in: Proceedings of the International Society of Magnetic Resonance in Medicine, 2006, p. 585.

[3] S.J. Kohler, Y. Yen, J. Wolber, R. Zandt, A. Gram, F. Ellner, M. Thanning, A. Chen, M. Albers, R. Bok, J. Tropp, S. Nelson, D. Vigneron, J. Kurhanewicz, Carbon-13 metabolic imaging at 3t using hyperpolarized ^{13}C-1 pyruvate, in: Proceedings of the International Society of Magnetic Resonance in Medicine, 2006, p. 586.

[4] M.S. Albert, G.D. Cates, B. Driehuys, W. Happer, B. Saam, C.S. Springer Jr., A. Wishnia, Biological magnetic resonance imaging using laser-polarized ^{129}Xe, Nature 370 (1994) 199–201 .

[5] J.R. MacFall, H.C. Charles, R.D. Black, H. Middleton, J.C. Swartz, B. Saam, B. Driehuys, C. Erickson, W. Happer, G.D. Cates, G.A. Johnson, C.E. Ravin, Human lung air spaces: potential for MR imaging with hyperpolarized He-3, Radiology 200 (1996) 553–558.

[6] R. Gruetter, I. Tkac, Field mapping without reference scan using asymmetric echo-planar techniques, Magn. Reson. Med. 43 (2000) 319–323.

[7] J. Magland, B. Vasilic, F.W. Wehrli, Fast low-angle dual spin-echo (flade): a new robust pulse sequence for structural imaging of trabecular bone, Magn. Reson. Med. 55 (2006) 465–471.

[8] S.M. Conolly, D.G. Nishimura, A. Macovski, A selective adiabatic spin-echo pulse, J. Magn. Reson. 83 (1989) 324–334.

[9] M.S. Silver, R.I. Joseph, D.I. Hoult, Selective spin inversion in nuclear magnetic resonance and coherent optics through an exact solution of the Bloch–Riccati equation, Phys. Rev. A 31 (1985) 2753–2755.

[10] J. Pauly, P. Le Roux, D. Nishimura, A. Macovski, Parameter relations for the Shinnar–Le Roux selective excitation pulse design algorithm, IEEE Trans. Med. Imaging 10 (1991) 53–65.

[11] C.H. Cunningham, D.B. Vigneron, A.P. Chen, D. Xu, S.J. Nelson, R.E. Hurd, D.A. Kelley, J.M. Pauly, Design of flyback echo-planar readout gradients for magnetic resonance spectroscopic imaging, Magn. Reson. Med. 54 (2005) 1286–1289.

[12] S.J. Nelson, Analysis of volume MRI and MR spectroscopic imaging data for the evaluation of patients with brain tumors, Magn. Reson. Med. 46 (2001).

[13] J.H. Ardenkjaer-Larson, B. Fridlund, A. Gram, G. Hansson, L. Hansson, M.H. Lerche, R. Servin, M. Thaning, K. Golman, Increase in signal-to-noise ration of >10,000 times in liquid-state NMR, Proc. Natl. Acad. Sci. USA 100 (2003) 10158–10163.